Journal of the Nigerian Mathematical Society
Vol. 32, pp. 33-60, 2013
©Nigerian Mathematical Society

ANALYTICAL SOLUTION TO MHD MICROPOLAR FLUID FLOW PAST A VERTICAL PLATE IN A SLIP-FLOW REGIME IN THE PRESENCE OF THERMAL DIFFUSION AND THERMAL RADIATION

J. I. OAHIMIRE, B. I. OLAJUWON[1], M. A WAHEED AND I. O. ABIALA

ABSTRACT. This present study investigates the effects of thermal-diffusion and thermal radiation on unsteady heat and mass transfer by free convective MHD micropolar fluid flow bounded by a semi- infinite vertical plate in a slip-flow regime under the action of transverse magnetic field with suction. The governing system of partial differential equations is transformed to dimensionless equations using dimensionless variables. The dimensionless equations are then solved analytically using perturbation technique to obtain expressions for velocity, microrotation, temperature and concentration. With the help of graphs, the effects of the various important parameters entering into the problem on the velocity, microrotation, temperature and concentration fields within the boundary layer are discussed. Also the effects of the pertinent parameters on the skin friction coefficient and rates of heat and mass transfer in terms of the Nusselt number and Sherwood numbers are presented numerically in tabular forms. The results shows that the observed parameters have significance influence on the flow, heat and mass transfer.

Keywords and phrases: Micropolar fluid, soret, perturbation technique, heat and mass transfer, slip-flow.
2010 Mathematical Subject Classification: 76Wxx, 76Dxx

1. INTRODUCTION

Micropolar fluids are subset of the micromorphic fluid theory introduced in a pioneering paper by Eringen[14]. Micropolar fluids are those fluids consisting of randomly oriented particles suspended in a viscous medium, which can undergo a rotation that can affect the hydrodynamics of the flow, making it a distinctly non- Newtonian fluid. They constitute an important branch of non-Newtonian fluid dynamics where microrotation effects as well as microinertia are exhibited. Eringen's theory has provided a good model for studying

Received by the editors May 6, 2012; Revised: July 8, 2012; Accepted: October 10, 2012
[1]Corresponding author

a number of complicated fluids, such as colloidal fluids, polymeric fluids and blood.

The effects of radiation on unsteady free convection flow and heat transfer problem have become more important industrially. At high operating temperature, radiation effect can be quite significant. Many processes in engineering areas occur at high temperature and a knowledge of radiation heat transfer becomes very important for design of reliable equipments, nuclear plants, gas turbines and various propulsion devices or aircraft, missiles, satellites and space vehicles. Based on these applications, Cogley et al.[13] showed that in the optically thin limit, the fluid does not absorb its own emitted radiation but the fluid does absorb radiation emitted by the boundaries. Hossain and Takhar[17] have considered the radiation effects on mixed convection boundary layer flow of an optically dense viscous incompressible fluid along a vertical plate with uniform surface temperature. Makinde[18] examined the transient free convection interaction with thermal radiation of an absorbing emitting fluid along moving vertical permeable plate. Satter and Hamid[16] investigated the unsteady free convection interaction with thermal radiation of an absorbing emitting plate. Rahman and Satter[4] studied transient convective flow of micropolar fluid past a continuous moving porous plate in the presence of radiation. Heat and mass transfer effects on unsteady magneto hydrodynamics free convection flow near a moving vertical plate embedded in a porous medium was presented by Das and Jana[19]. Olajuwon[15] examine convection heat and mass transfer in a hydromagnetic flow of a second grade fluid past a semi-infinite stretching sheet in the presence of thermal radiation and thermal diffusion. Haque et al.[20] studied micropolar fluid behavior on steady magneto hydrodynamics free convection flow and mass transfer through a porous medium with heat and mass fluxes. Soret and Dufour effects on mixed convection in a non- Darcy porous medium saturated with micropolar fluid was studied by Srinivasacharya[12]. Rebhi[9] studied unsteady natural convection heat and mass transfer of micropolar fluid over a vertical surface with constant heat flux. The governing equations were solved numerically using McCormack's technique and the effects of various parameters were investigated on the flow. Eldabe and Ouaf[6] solved the problem of heat and mass transfer in a hydromagnetic flow of a micropolar fluid past a stretching surface with ohmic heating and viscous dissipation using the Chebyshev finite difference method. Keelson and Desseaux[5] studied the effect of surface

conditions on the flow of a micropolar fluid driven by a porous stretching surface. The governing equations were solved numerically. Sunil et al.[1] studied the effect of rotation on a layer of micropolar ferromagnetic fluid heated from below saturating a porous medium. The resulting non-linear coupled differential equations from the transformation were solved using finite-difference method. Mahmoud [7] investigated thermal radiation effect on magneto hydrodynamic flow of a micropolar fluid over a stretching surface with variable thermal conductivity. The solution was obtained numerically by iterative, Runge-Kuta order-four method. Magdy[10] studied unsteady free convection flow of an incompressible electrically conducting micropolar fluid, bounded by an infinite vertical plane surface of constant temperature with thermal relaxation including heat sources. The governing equations were solved using Laplace transformation. The inversion of the Laplace transforms was carried out with a numerical method. The obtained self-similar equation were solved numerically by an efficient implicit, iterative, infinite-difference method. Reena and Rana[8] investigated double-diffusive convection in a micropolar fluid layer heated and soluted from below saturating a porous medium. A linear stability analysis theory and normal mode analysis method was used. Kandasamy et al. [22] studied the nonlinear MHD flow, with heat and mass transfer characteristics, of an incompressible, viscous, electrically conducting, Boussinesq fluid on a vertical stretching surface with chemical reaction and thermal stratification effects. Modather et al. [21] studied MHD heat and mass transfer oscillatory flow of a micropolar fluid over a vertical permeable plate in a porous medium. Seddek [26] studied the effects of chemical reaction, thermophoresis and variable viscosity on steady hydromagnetic flow with heat and mass transfer over a flat plate in the presence of heat generation/absorption. Patil and Kulkarni[3] studied the effects of chemical reaction flow of a polar fluid through porous medium in the presence of internal heat generation. Double-diffusive convection radiation interaction on unsteady MHD flow over a vertical moving porous plate with heat generation and soret effects was studied by Mohamed[23]. Khedr et al.[25] studied MHD flow of a micropolar fluid past a stretched permeable surface with heat generation or absorption. Unsteady free convection non-Newtonian fluids have many applications in geophysics, turbomachinery and many other fields. Chaudhary[27] studied the effect of chemical reactions on MHD micropolar fluid flow past a vertical plate in slip-flow regime.

When heat and mass transfer occur simultaneously in a moving fluid, the relations between the fluxes and the driven potential are important. It has been found that an energy flux can be generated not only by temperature gradients but by composition gradient as well. The energy caused by a composition gradient is called the Dufour or the diffusion-thermo effect, also the mass fluxes can also be caused by the temperature gradient and this is called the Soret or thermal diffusion effect, the diffusion-thermo effect is neglected in this study because it is of a smaller order of magnitude than the magnitude of thermal radiation which exerts a stronger effect on the energy flux. Thermal diffusion effect or Soret effect has been utilized for isotope separation in mixtures between gases with very light molecular weight (H_2, He) and medium molecular weight (N_2, air) and it was found to be of a magnitude that it cannot be neglected due to its practical applications in engineering and sciences. For some industrial applications such as glass production and furnace design, and in space technology applications such as cosmical flight aerodynamics rocket and spacecraft re-entry aerothermodynamics which operate at higher temperature, thermal radiation effect can be significant.

This paper extends the works of Chaudhary[27] by examining the combine effects of chemical reaction, thermal diffusion and thermal radiation on unsteady free convection heat and mass transfer flow of a micropolar fluid past a vertical porous plate in a slip-flow regime with suction. The governing equations are solved analytically using perturbation method. Analysis and discussions of the results were carried out using the different values of the parameters embedded in the system. These results were further presented in tabular and graphical forms.

2. MATHEMATICAL FORMULATION

e consider unsteady viscous incompressible and electrically conducting two dimensional flow of a micropolar fluid past a semi-infinite vertical plate embedded in a porous medium in the slip-flow regime. The x- axis is taken along the porous plate in the upward direction and y-axis normal to it as shown in fig.1 below:

The surface of the plate is held at a constant heat flux q_w, and the mass flux of a certain constituent in the solution that saturated the porous medium is held at m_w near the surface. Due to the semi-infinite plane surface assumption, the flow variables are functions of y and t only . It is assumed that there is no applied voltage which

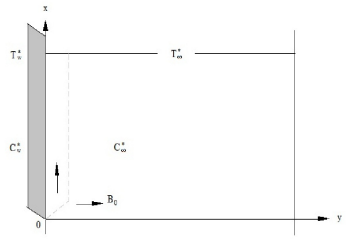

Fig. 1. Physical model

implies the absence of an electric field. We choose the coordinate system such that x-axis is along the vertical plate and y-axis normal to the plate. It is assumed that the induced magnetic field is neglected compared to the applied magnetic field. The effect of the viscous dissipation is negligible in the energy equation and there is a first order chemical reaction between the diffusing species and the fluid.

Under these assumptions, the governing equation of the flow are:

$$\frac{\partial v^*}{\partial y^*} = 0, \tag{1}$$

$$\begin{aligned} \frac{\partial u^*}{\partial t^*} + v^*\frac{\partial u^*}{\partial y^*} &= -\frac{1}{\rho}\frac{\partial p^*}{\partial x^*} + (\nu+\nu_r)\frac{\partial^2 u^*}{\partial y^{*2}} + g\beta_f(T^*-T^*_\infty) \\ &\quad + g\beta_c(C^*-C^*_\infty) - \frac{\nu u^*}{K^*} - \sigma\frac{B_o^2 u^*}{\rho} + 2\nu_r\frac{\partial w^*}{\partial y^*} \end{aligned} \tag{2}$$

$$\rho j^*\left(\frac{\partial w^*}{\partial t^*} + v^*\frac{\partial w^*}{\partial y^*}\right) = \gamma\frac{\partial^2 w^*}{\partial y^*}, \tag{3}$$

$$\frac{\partial T^*}{\partial t^*} + v^*\frac{\partial T^*}{\partial y^*} = \alpha\frac{\partial^2 T^*}{\partial y^{*2}} - \frac{1}{\rho C_p}\frac{\partial q_r}{\partial y^*}, \tag{4}$$

$$\frac{\partial C^*}{\partial t^*} + v^*\frac{\partial C^*}{\partial y^*} = D^*\frac{\partial^2 C^*}{\partial y^{*2}} - K_c^*(C^*-C^*_\infty) + D^*\frac{K_T}{T_m}\frac{\partial^2 T^*}{\partial y^{*2}}. \tag{5}$$

It is assumed that the free stream velocity U^*_∞ follows an exponentially small perturbation law. Under these assumptions, the appropriate boundary conditions are:

$$u^* = U_0 + L_1^*\frac{\partial u^*}{\partial y^*}, T^* = T^*_w, w^* = -n\frac{\partial u^*}{\partial y^*}, C^* = C^*_w, at\ y^* = 0, \tag{6}$$

$$\begin{aligned} u^* \to U^*_\infty &= U_0\left(1+\epsilon e^{\delta^* t^*}\right), T^* \to T^*_\infty, w^* \to 0, \\ &\quad C^* \to C^*_\infty, at\ y^* \to \infty. \end{aligned} \tag{7}$$

Where $L_1^* = \left(\frac{2-m_1}{m_1}\right)$,$L^*$ being the mean free path and m_1 the Maxwell's reflection coefficient,ϵ and δ^* are less than unity. The boundary conditions for microrotation variable w^* describe the relationship with surface stress. In this equation, parameter n is a number between 0 and 1 that relates the microrotation gyration vector to the shear stress. The value n=0 corresponds to the case where the particle density is sufficiently large so that microelements close to the wall are unable to rotate. The value n=0.5 is indicative of the weak concentration, and when n=1, flows are believed to represent the turbulent boundary layer(Rees and Basson[28]).
Integrating the continuity equation (1), v^* is either constant or function of time, the suction normal to the plate can be written as

$$v^* = -V_0 \left(1 + \epsilon A e^{\delta^* t^*}\right). \tag{8}$$

Where A is a real positive constant and ϵA is less than unity,V_0 is the scale of the suction velocity which has a non-zero positive constant. Following Chaudhary[27], the pressure gradient takes the form:

$$-\frac{1}{\rho}\frac{\partial p^*}{\partial x^*} = \frac{dU_\infty^*}{dt^*} + \frac{\nu}{K^*}U_\infty^* + \frac{\sigma}{\rho}B_0^2 U_\infty^*. \tag{9}$$

Following Rosseland approximation (Brewstar[11]) the radiative heat flux q_r is modeled as

$$q_r = -\frac{4\sigma^*}{3k^*}\frac{\partial T^{*4}}{\partial y^*}. \tag{10}$$

Where σ^* is the Stefan-Boltzman constant and k^* is the mean absorption coefficient. Assuming that the difference in temperature within the flow are such that T^{*4} can be expressed as a linear combination of the temperature, we expand T^{*4} in Taylor's series about T_∞^* as follows

$$T^{*4} = T_\infty^{*4} + 4T_\infty^{*3}(T^* - T_\infty^*) + 6T_\infty^{*2}(T^* - T_\infty^*)^2 + ..., \tag{11}$$

and neglecting higher order terms beyond the first degree in$(T^* - T_\infty^*)$, we have

$$T^{*4} \approx -3T_\infty^{*4} + 4T_\infty^{*3}T^*, \tag{12}$$

Differentiating equation (10) with respect to y^* and using equation(12) to obtain

$$\frac{\partial q_r}{\partial y^*} = -\frac{16T_\infty^{*3}\sigma^*}{3k^*}\frac{\partial^2 T^*}{\partial y^{*2}} \tag{13}$$

Let us introduce the following dimensionless variables:

$$u = \frac{u^*}{U_0}, v = \frac{v^*}{V_0}, y = \frac{V_0 y^*}{\nu}, U_\infty = \frac{U_\infty^*}{V_0}, w = \frac{\nu}{U_0 V_0} w^*, t = \frac{t^*}{\nu} V_0^2, \tag{14}$$

$$\theta = \frac{T^* - T_\infty^*}{T_w^* - T_\infty^*}, C = \frac{C^* - C_\infty^*}{C_w^* - C_\infty^*}, \delta = \frac{\delta^*}{V_0^2}\nu, K = \frac{K^* V_0^2}{\nu^2}, J = \frac{J^*}{\nu^2} V_0^2. \tag{15}$$

Substituting equation (14) and (15) into equations (2) - (5) yield the following dimensionless equations:

$$\begin{aligned} \frac{\partial u}{\partial t} - \left(1 + \epsilon A e^{\delta t}\right) \frac{\partial u}{\partial y} &= \frac{dU_\infty}{dt} + (1+\beta)\frac{\partial^2 u}{\partial y^2} + G_r \theta \\ &\quad + G_r c C + N(U_\infty - u) + 2\beta \frac{\partial w}{\partial y}, \end{aligned} \tag{16}$$

$$\frac{\partial w}{\partial t} - \left(1 + \epsilon A e^{\delta t}\right) \frac{\partial w}{\partial y} = \frac{1}{\eta}\frac{\partial^2 w}{\partial y^2}, \tag{17}$$

$$\frac{\partial \theta}{\partial t} - \left(1 + \epsilon A e^{\delta t}\right) \frac{\partial \theta}{\partial y} = \frac{1}{Pr}(1 + N_r)\frac{\partial^2 \theta}{\partial y^2}, \tag{18}$$

$$\frac{\partial C}{\partial t} - \left(1 + \epsilon A e^{\delta t}\right) \frac{\partial C}{\partial y} = \frac{1}{Sc}\frac{\partial^2 C}{\partial y^2} - K_c C + Sr \frac{\partial^2 \theta}{\partial y^2}. \tag{19}$$

Where $N = (M + \frac{1}{K})$, $\eta = \frac{\mu j^*}{\gamma} = \frac{2}{2+\beta}$ and $M = \frac{\sigma B_o^2 \nu}{\rho \nu_o^2}$, the magnetic field parameter, $Gr = \frac{\nu \beta_f g (T_w^* - T_\infty^*)}{U_o^2 V_o^2}$ the Grashot number, $G_r c = \frac{\nu \beta_c (C_w^* - C_\infty^*)}{U_o^2 V_o^2}$ the mogified Grashof number, $Pr = \frac{\nu \rho C_p}{k}$ the Prandtl number, $Sc = \frac{\nu}{D}$ the Schmidt number, $h = \frac{V_0 L^*}{\gamma}$ the refraction parameter,$Sr = \frac{D^* K_T}{T_m} \frac{(T_w^* - T_\infty^*)}{\nu (C_w^* - C_\infty^*)}$ the soret number,$K_c = \frac{K_c^* \nu}{V_0^2}$ chemical reaction parameter and $Nr = \frac{16 T_\infty^* \sigma^*}{3 k^* k}$ the radiation parameter.

$$u = 1 + h\frac{\partial u}{\partial y}, \theta = 1, w = -n\frac{\partial u}{\partial y}, C = 1 at y = 0, \tag{20}$$

$$u \to U_\infty, \theta \to 0, w \to 0, C \to 0, as, y \to \infty. \tag{21}$$

The local skin friction coefficient, couple stress coefficient, Nusselt number and Sherwood number are important physical quantities of engineering interest. The skin friction coefficient(Cf) at the wall is

given by

$$\begin{aligned} Cf &= \frac{2\tau_w}{\rho U_0 V_0} = 2(1+(1-n)\beta)u'(0) = 2(1+(1-n)\beta)(b_2A_1 \\ &\quad +aA_3 + b_1A_4 + \eta A_5 + \epsilon e^{\delta t}(b_6A_6 + b_3A_8 + aA_9 + \\ &\quad b_4A_{10} + b_1A_{11} + b_5A_{12} + \eta A_{13} + b_2A_{14})), \end{aligned} \tag{22}$$

The couple stress coefficient (Cm) at the plate is written as

$$Cm = \frac{M_w}{\mu J U_0} = (1+\frac{\beta}{2})w'(0) = -(1+\frac{\beta}{2})(\eta B_1 + \epsilon e^{\delta t}(b_5B_2 + \eta B_3), \tag{23}$$

The rate of heat transfer in terms of the Nusselt number is given by

$$Nu = \frac{q_w^*\nu}{kU_0^*(T_w^* - T_\infty^*)} = -\frac{\partial\theta}{\partial y}(at, y=0) = (a + \epsilon e^{\delta t}(b_3D_1 + aD_2), \tag{24}$$

The coefficient of mass transfer, which is generally know as Sherwood number is given by

$$\begin{aligned} Sh &= \frac{J^*\nu}{U_0\rho D(C_w^* - C_\infty^*)} = -\frac{\partial C}{\partial y}(at, y=0) \\ &= (b_1E_1 + aE_2 + \epsilon e^{\delta t}(b_4E_3 + b_1E_4 + aE_5 + b_3E_6)). \end{aligned} \tag{25}$$

3. METHOD OF SOLUTION

To find the analytical solution of the above system of partial differential equations (16) - (19) under the above boundary conditions (20), (21), we assume a perturbation of the form:

$$u = u_0(y) + \epsilon e^{\delta t}u_1(y) + o(\epsilon^2), \tag{26}$$

$$w = w_0(y) + \epsilon e^{\delta t}w_1(y) + o(\epsilon^2), \tag{27}$$

$$\theta = \theta_0(y) + \epsilon e^{\delta t}\theta_1(y) + o(\epsilon^2), \tag{28}$$

$$C = u_0(y) + \epsilon e^{\delta t}C_1(y) + o(\epsilon^2). \tag{29}$$

Substituting equations (26) - (29) into equations (16) - (19) , neglecting the higher order terms of $O(\epsilon^2)$ to obtain the following set of equations:

$$(1+\beta)u_0'' + u_0' - Nu_0 = -N - G_r\theta_0 + G_rcC_0 - 2\beta w_0', \tag{30}$$

$$(1+\beta)u_1'' + u_1' - (N+\delta)u_1 = -(N+\delta) - G_r\theta_1 + G_rcC_1 - 2\beta w_1' - Au_0', \tag{31}$$

$$w_0'' + \eta w_0' = 0, \tag{32}$$

$$w_1'' + \eta w_1' - \delta\eta w_1 = -A\eta w_0', \tag{33}$$

$$\theta_0'' + a\theta_0' = 0, \tag{34}$$

$$\theta_1'' + a\theta_1' - a\delta\theta_1 = -aA\theta_0', \tag{35}$$

$$C_0'' + ScC_0' - K_cScC_0 = -ScSr\theta_0'', \tag{36}$$

$$C_1'' + ScC_1' - (\delta + K_c)ScC_1 = -AScC_0' - ScSr\theta_1'' \tag{37}$$

Where a=Pr/(1+Nr)

The corresponding boundary conditions can be written as

$$\begin{aligned} u_0 &= 1 + h\frac{\partial u_0}{\partial y}, u_1 = h\frac{\partial u_1}{\partial y}, w_0 = -nu_0', w_1 = -nu_1', \\ &\theta_0 = 1, \theta_1 = 0, C_0 = 1, C_1 = 0, at, y = 0, \end{aligned} \tag{38}$$

$$\begin{aligned} u_0 &= 1, u_1 = 1, w_0 = 0, w_1 = 0, \theta_0 = 0, \theta_1 = 0, C_0 = 0, \\ &C_1 = 0, at, y \to \infty. \end{aligned} \tag{39}$$

The solution of (30) - (37) satisfying the boundary conditions (38) and (39) are given by

$$\begin{aligned} u &= 1 + A_1e^{-b_2y} + A_3e^{-ay} + A_4e^{-b_1y} + A_5e^{-\eta y} + \epsilon e^{\delta t}(1 + A_6e^{-b_6y} \\ &+A_8e^{-b_3y} + A_9e^{-ay} + A_{10}e^{-b_4y} + A_{11}e^{-b_1y} + A_{12}e^{-b_5y} \\ &+A_{13}e^{-\eta y} + A_{14}e^{-b_2y}), \end{aligned} \tag{40}$$

$$w = B_1e^{-\eta y} + \epsilon e^{\delta t}(B_2e^{-b_5y} + B_3e^{-\eta y}), \tag{41}$$

$$\theta = e^{-ay} + \epsilon e^{\delta t}(D_1e^{-b_3y} + D_2e^{-ay}), \tag{42}$$

$$C = E_1e^{-b_1y} + E_2e^{-ay} + \epsilon e^{\delta t}(E_3e^{-b_4y} + E_4e^{-b_1y} + E_5e^{-ay} + E_6e^{-b_3y}). \tag{43}$$

Where

$$
\begin{aligned}
b_1 &= \tfrac{Sc+\sqrt{Sc^2+4K_cSc}}{2}\\
b_2 &= \tfrac{1+\sqrt{1+4(1+\beta)N}}{2(1+\beta)}\\
b_3 &= \tfrac{a+\sqrt{a^2+4a\delta}}{2}\\
b_4 &= \tfrac{Sc+\sqrt{Sc^2+4(\delta+K_c)Sc}}{2}\\
b_5 &= \tfrac{\eta+\sqrt{\eta^2+4\delta\eta}}{2}\\
b_6 &= \tfrac{1+\sqrt{1+4(1+\beta)(N+\delta)}}{2}\\
E_2 &= \tfrac{-ScSr}{a^2-aSc-K_cSc}\\
E_1 &= 1-E_2\\
A_3 &= \tfrac{-(Gr+GrcE_2)}{((1+\beta)a^2-a-N)}\\
A_4 &= \tfrac{-GrcE_1}{(1+\beta)b_1^2-b_1-N}\\
A_5 &= [2\beta\eta[(naA_3+nb_1A_4)(1+hb_1)-(nb_2(A_3(ha+1)\\
&\quad +A_4(hb_1+1))]]/[([((1+\beta)\eta^2-\eta-N)\\
&\quad -2\beta n\eta^2](1+ha)+2\beta\eta nb_2(h\eta+1))]\\
A_1 &= \tfrac{-[A_3(ha+1)+A_4(hb_1+1)+A_5(h\eta+1)}{(1+hb_1)}\\
B_1 &= n(b_2A_1+aA_3+b_1A_4+\eta A_5)\\
D_2 &= \tfrac{-aA}{\delta}\\
D_1 &= -D_2\\
E_4 &= \tfrac{AScb_1E_1}{b_1^2-b_1Sc-(\delta+K_c)Sc}\\
E_5 &= \tfrac{AScaE_2-ScSra^2D_2}{a^2-aSc-(\delta+K_c)Sc}\\
E_6 &= \tfrac{-ScSrb_3^2D_1)}{b_3^2-b_3Sc-(\delta+K_c)Sc}\\
E_3 &= -(E_4+E_5+E_6)\\
B_3 &= \tfrac{-AetaB_1}{\delta}\\
A_8 &= \tfrac{-(GrD_1+GrcE_6)}{(1+\beta)b_3^2-b_3-(N+\delta)}\\
A_9 &= \tfrac{AaA_3-(GrD_2+GrcE_5)}{(1+\beta)a^2-a-(N+\delta)}\\
A_{10} &= \tfrac{-GrcE_3}{(1+\beta)b_4^2-b_4-(N+\delta)}\\
A_{11} &= \tfrac{Ab_1A_4-GrcE_4}{(1+\beta)b_1^2-b_1-(N+\delta)}\\
A_{13} &= \tfrac{2\beta\eta B_3+A\eta A_5}{(1+\beta)\eta^2-\eta-(N+\delta)}\\
A_{12} &= [2\beta b_5((hb_6+1)(nb_3A_8+naA_9+nb_4A_{10}+nb_1A_{11}\\
&\quad +n\eta A_{13}+nb_2A_{14}-B_3)-nb_6(A_8(hb_3+1)\\
&\quad +A_9(ha+1)+A_{10}(hb_4+1)+A_{11}\\
&\quad (hb_1+1)+A_{13}(h\eta+1)+A_{14}(hb_2+1)))]/\\
&\quad [(hb_6+1)[((1+\beta)b_5^2-b_5-(N+\delta))\\
&\quad +2\beta b_5(nb_6-nb_5)]
\end{aligned}
$$

4. RESULTS

The results are presented as velocity, microrotation, temperature and concentration profiles in figures 2 - 28 and tables 1-5 below:

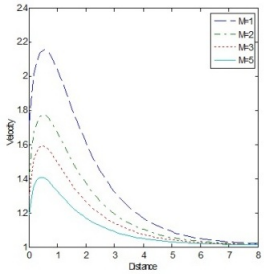

Fig. 2. Velocity profiles for different values of M with $\beta = 0.5$, $n = 0.5$, $Sc = 1$,$K = 2$,$Kc = 2$,$Gr = 2$,$Grc = 2$,$Pr = 1$, $h = 0.4$,A=0.5,t=1, M=2, Nr=0.5,Sr=2.

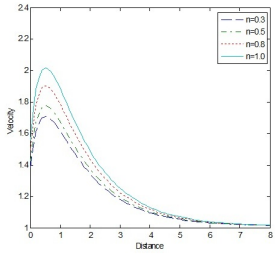

Fig. 3. Velocity profiles for different values of n with $\beta = 0.5$, Sc=1,K=2,Kc=2,Gr=2,Grc=2,Pr=1, h=0.4,A=0.5,t=1, M=2,Nr=0.5,Sr=2.

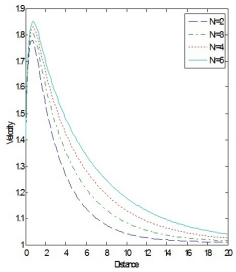

Fig. 4. Velocity profiles for different values of Nr with $\beta = 0.5$, Sc=1,K=2,Kc=2,Gr=2,Grc=2,Pr=1, h=0.4,A=0.5,t=1, M=2,n=0.5,Sr=2.

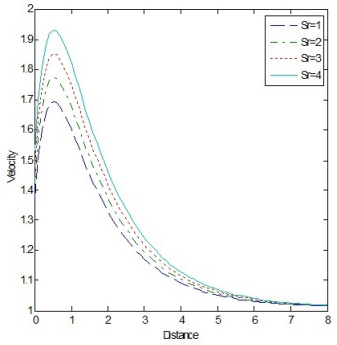

Fig. 5. Velocity profiles for different values of Sr with $\beta = 0.5$, n=0.5, Sc=1,K=2,Kc=2,Gr=2,Grc=2,Pr=1, h=0.4,A=0.5,t=1, M=2,Nr=0.5.

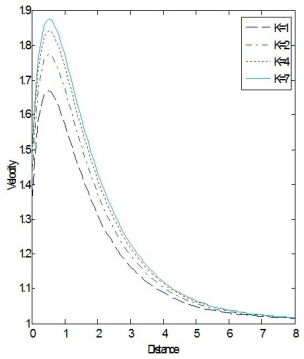

Fig. 6. Velocity profiles for different values of K with $\beta = 0.5$, n=0.5, Sc=1,Kc=2,Gr=2,Grc=2,Pr=1, h=0.4,A=0.5,t=1, M=2,Nr=0.5,Sr=2.

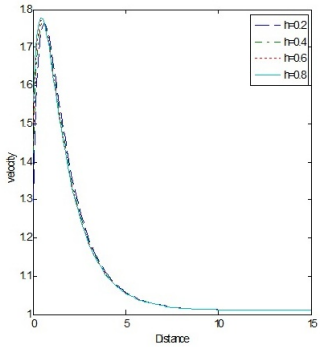

Fig. 7. Velocity profiles for different values of h with $\beta = 0.5$, n=0.5, Sc=1,K=2,Kc=2,Gr=2,Grc=2,Pr=1, 4,A=0.5,t=1, M=2,Nr=0.5,Sr=2.

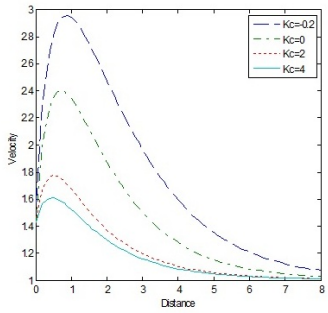

Fig. 8. Velocity profiles for different values of K_c with $\beta = 0.5$, n=0.5, Sc=1,K=2,Kc=2,Gr=2,Grc=2,Pr=1, h=0.4,A=0.5,t=1, M=2,Nr=0.5,Sr=2.

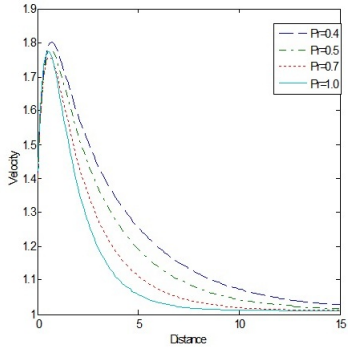

Fig. 9. Velocity profiles for different values of Pr with $\beta = 0.5$, n=0.5, Sc=1,K=2,Kc=2,Gr=2,Grc=2,Pr=1, h=0.4,A=0.5,t=1, M=2,Nr=0.5,Sr=2.

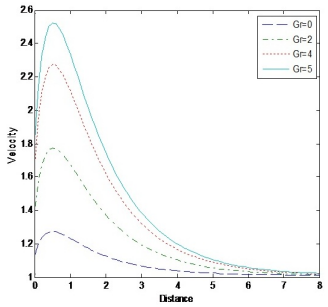

Fig. 10. Velocity profiles for different values of Gr with β=0.5, n=0.5, Sc=1,K=2,Kc=2,Grc=2,Pr=1, h=0.4,A=0.5,t=1, M=2,Nr=0.5,Sr=2.

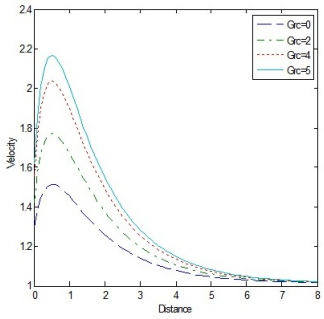

Fig. 11. Velocity profiles for different values of Gc with $\beta = 0.5$, n=0.5, Sc=1,K=2,Kc=2,Gr=2,A=0.5,t=1,Pr=1,h=0.4, M=2,Nr=0.5,Sr=2.

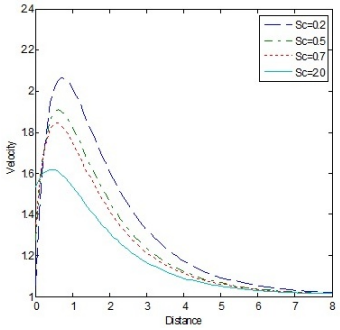

Fig. 12. Velocity profiles for different values of Sc with $\beta = 0.5$, n=0.5, K=2,Kc=2,Gr=2,Grc=2,Pr=1, h=0.4,A=0.5,t=1, M=2,Nr=0.5,Sr=2.

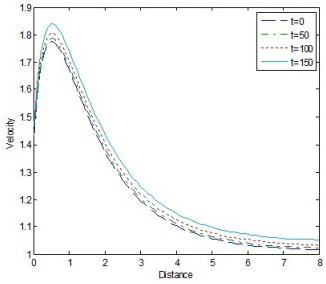

Fig. 13. Velocity profiles for different values of t with $\beta = 0.5$, n=0.5, Sc=1,K=2,Kc=2,Gr=2,Grc=2,Pr=1, h=0.4,A=0.5, M=2, Nr=0.5,Sr=2.

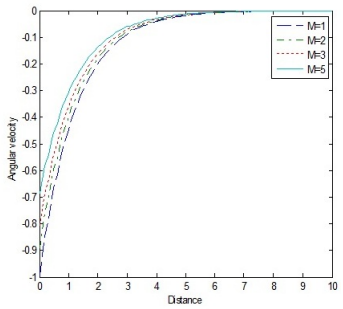

Fig. 14. Microrotation profiles for different values of M with $\beta = 0.5$, n=0.5, Sc=1,K=2,Kc=2,Gr=2,Grc=2,Pr=1, h=0.4,A=0.5,t=1, Nr=0.5,Sr=2.

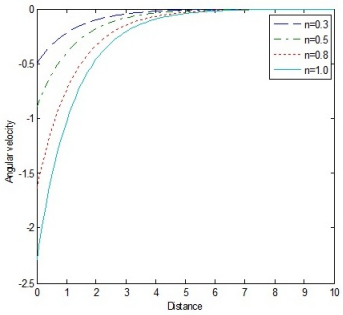

Fig. 15. Microrotation profiles for different values of n with $\beta = 0.5$, Sc=1,K=2,Kc=2,Gr=2,Grc=2,Pr=1, h=0.4,A=0.5,t=1, M=2,Nr=0.5,Sr=2.

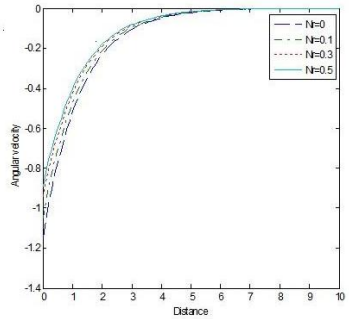

Fig. 16. Microrotation profiles for different values of Nr with $\beta = 0.5$, n=0.5, Sc=1,K=2,Kc=2,Gr=2,Grc=2,Pr=1, h=0.4,A=0.5,t=1, M=2,Sr=2.

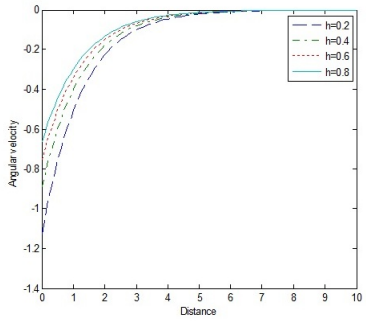

Fig. 17. Microrotation profiles for different values of h with $\beta = 0.5$, n=0.5, Sc=1,K=2,Kc=2,Gr=2,Grc=2,Pr=1, A=0.5,t=1, M=2,Nr=0.5,Sr=2.

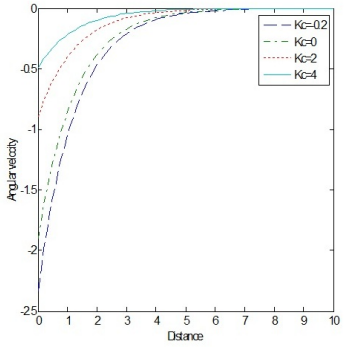

Fig. 18. Microrotation for different values of K_c with $\beta = 0.5$, n=0.5, Sc=1,K=2,Gr=2,Grc=2,Pr=1, h=0.4,A=0.5,t=1, M=2,Nr=0.5,Sr=2.

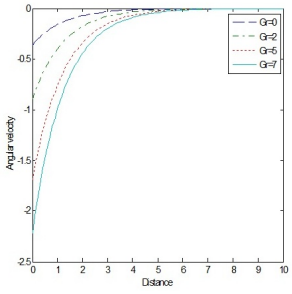

Fig. 19. Microrotation profiles for different values of Gr with $\beta = 0.5$, n=0.5, Sc=1,K=2,Kc=2,Grc=2,Pr=1, h=0.4,A=0.5,t=1, M=2,Nr=0.5,Sr=2.

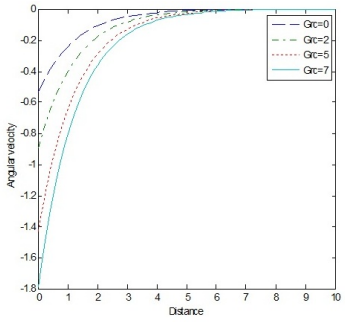

Fig. 20. Microrotation profiles for different values of Gc with $\beta = 0.5$, n=0.5, Sc=1,K=2,Kc=2,Gr=2,Pr=1, h=0.4,A=0.5,t=1, M=2,Nr=0.5,Sr=2.

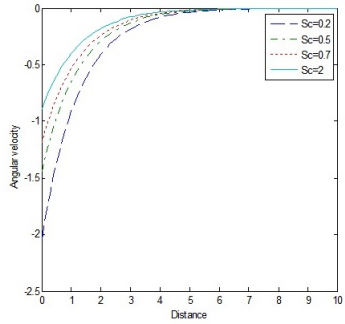

Fig. 21. Microrotation profiles for different values of Sc with $\beta = 0.5$, n=0.5, K=2,Kc=2,Gr=2,Grc=2,Pr=1, h=0.4,A=0.5,t=1, M=2,Nr=0.5,Sr=2.

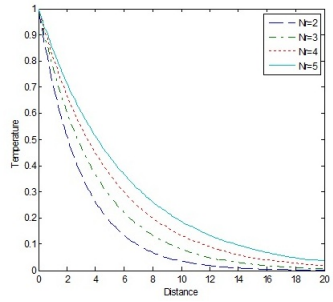

Fig. 22. Temperature profiles for different values of Nr with $\beta = 0.5$, n=0.5, Sc=1,K=2,Kc=2,Gr=2,Grc=2,Pr=1, h=0.4,A=0.5,t=1, M=2,Sr=2.

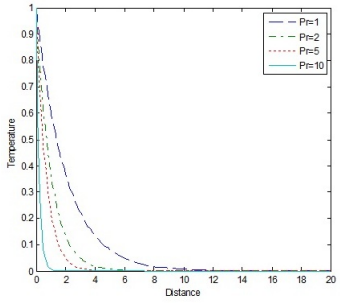

Fig. 23. Temperature profiles for different values of Pr with $\beta = 0.5$, n=0.5, Sc=1,K=2,Kc=2,Gr=2,Grc=2, h=0.4,A=0.5,t=1, M=2,Nr=0.5,Sr=2

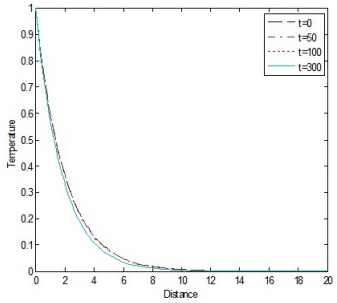

Fig. 24. Temperature profiles for different values of t with $\beta = 0.5$, n=0.5, Sc=1,K=2,Kc=2,Gr=2,Grc=2,Pr=1, h=0.4,A=0.5, M=2, Nr=0.5,Sr=2

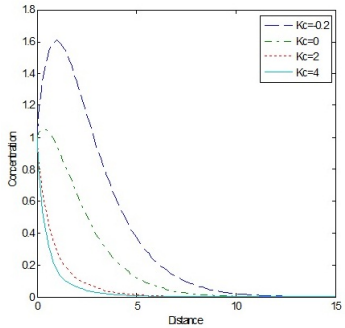

Fig. 25. Concentration profiles for different values of K_c with $\beta = 0.5$, n=0.5, Sc=1,K=2,Gr=2,Grc=2,Pr=1, h=0.4,A=0.5,t=1, M=2,Nr=0.5,Sr=2.

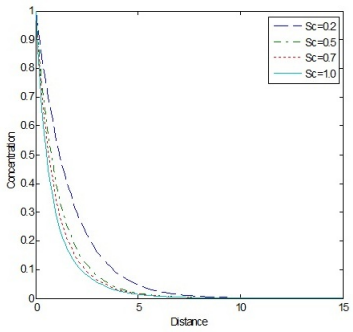

Fig. 26. Concentration profiles for different values of Sc with $\beta = 0.5$, n=0.5, K=2,Kc=2,Gr=2,Grc=2,Pr=1, h=0.4,A=0.5,t=1, M=2,Nr=0.5,Sr=2.

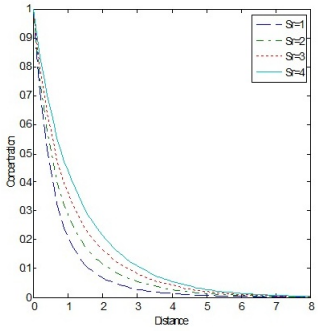

Fig. 27. Concentration profiles for different values of Sr with $\beta = 0.5$, n=0.5, Sc=1,K=2,Kc=2,Gr=2,Grc=2,Pr=1, h=0.4,A=0.5,t=1, M=2,Nr=0.5

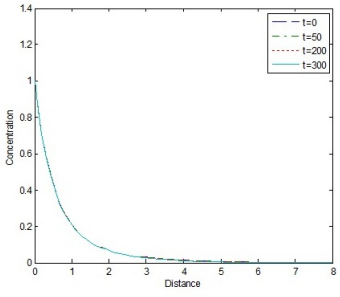

Fig. 28. Concentration profiles for different values of t with $\beta = 0.5$, n=0.5, Sc=1,K=2,Kc=2,Gr=2,Grc=2,Pr=1, h=0.4,A=0.5,t=1, M=2, Nr=0.5,Sr=2.

Table 1. Effect of various parameter on Cf with,$\beta = 0.5$, n=0.5, K=2, Gr=2,Grc=2, M=2, Pr=1,Sr=2, A=0.5, t=1, h=0.4

Sc	Nr	Kc	Sr	Cf
0.2	0.5	2	2	4.2758
0.5	0.5	2	2	3.1592
1	0.5	2	2	0.0423
1	1	2	2	1.8372
1	2	2	2	1.8663
1	3	2	2	1.9035
1	0.5	-0.2	2	5.3315
1	0.5	2	2	4.3413
1	0.5	2	2	1.8915
1	0.5	2	1	1.6869
1	0.5	2	1.5	1.7892
1	0.5	2	2	1.8915

Table 2. Effect of various parameter on Cm ,with $\beta = 0.5$ n=0.5, K=2, Gr=2,Grc=2, M=2, Pr=1,Sr=2, A=0.5, t=1, h=0.4

Sc	Nr	Kc	Sr	Cm
0.2	0.5	2	2	-0.5897
0.5	0.5	2	2	-0.7096
1	0.5	2	2	-0.9544
1	1	2	2	-0.8334
1	2	2	2	-0.8288
1	3	2	2	-0.8254
1	0.5	-0.2	2	-0.5309
1	0.5	2	2	-0.6181
1	0.5	2	2	-0.8290
1	0.5	2	1	-0.8325
1	0.5	2	1.5	-0.8267
1	0.5	2	2	-0.8209

Table 3. Effect of Pr and Nr on Nu, with, $\beta = 0.5$ n=0.5, K=2, Gr=2,Grc=2, M=2, Sr=2, A=0.5, t=1, h=0.4

Pr	Nr	Nu
2	0.5	1.3400
3	0.5	2.0101
7	0.5	4.6903
1	1	0.5025
1	2	0.3350
1	3	0.2512

Table 4. Effect of Kc and Sc on Sh with,$\beta = 0.5$ n=0.5, K=2, Gr=2,Grc=2, M=2, Pr=1,Sr=2, A=0.5, t=1, h=0.4

Kc	Sc	Sh
-0.2	2	-2.2410
0	2	-0.6701
2	2	2.3000
2	1	1.4652
2	1.5	1.8968
2	2	2.3000

Table 5. Variation of time on Cf , Nu and Sh with $\beta = 0.5$ =0.5, n=0.5, Sc=1,K=2,Kc=2,Gr=2,Grc=2,Pr=1, h=0.4,A=0.5, M=2,Nr=0.5

t	Cf	Nu	Sh
0	1.1338	0.6700	2.3000
10	1.1340	0.6703	2.2998
50	1.1346	0.6721	2.2989
100	1.1359	0.6756	2.2970
150	1.1380	0.6814	2.2940
200	1.1415	0.6909	2.2889

5. DISCUSSON

We have formulated the convective MHD micropolar fluid flow bounded by a semi-infinite vertical plate in a porous medium. This enables us to carry out the numerical calculations for the distribution of the translational velocity, microrotation, temperature and concentration across the boundary layer for various values of parameters. In this study,we have chosen $\epsilon = 0.01$, $\delta = 0.01$, A=0.5,

$\beta = 0.5$ while Nr, Sr, Sc, M, Gr, Grc, K, Pr, h, Kc, t and K are varied over a range. The effect of magnetic field parameter on translational velocity across the boundary layer are presented in figure2. It is obvious that the effect of increasing values of the magnetic field parameter M results in a decreasing velocity distribution across the boundary layer. This is due to the fact that the introduction of transverse magnetic field normal to the flow direction has a tendency to create a drag force due to Lorentz force and hence results in retarding the velocity profiles. Figure3 shows the effect of the parameter which relates to the microgyration vector and the shear stress on the translational velocity. It is observed that the translational velocity increases with increasing values of the parameter n. Figure4 shows the translational velocity distribution across the boundary layer for different values of the thermal radiation parameter Nr. The figure indicates that velocity profiles increases as the radiation parametrer increases and as a result, the momentum boundary layer thickness increases. This is because when the intensity of heat generated through thermal radiation increased, the bond holding the components of the fluid particle is easily broken and the fluid velocity will increased. Figure5 illustrates the variation of the translational velocity distribution across the boundary layer for various values of Soret parameter Sr. It is clear that the translational velocity of the fluid flow increases with increase in the Soret parameter. Thus the effect of increasing values of the Soret parameter Sr is to increase the momentum boundary layer thickness. For various values of the permeability of the porous medium(K), the profiles of the translational velocity is shown in figure6. The translational velocity increases for increasing values of the permeability parameter. Figure7 depicts the translational velocity for different values of refraction parameter (h). It can be observed from the figure that the velocity increases with increasing values of the refraction parameter h near the plate and start decreasing away from the plate. Figure8 illustrates the variation in velocity distribution across the boundary layer for various values of the chemical reaction parameter (Kc). It can be seen that the translational velocity increases during the generative reaction ($Kc < 0$) and decreases in the destructive reaction ($Kc > 0$). Figure9 present the velocity profiles for different values of the Prandtl number Pr. The results shows that the effect of increasing values of Pr results in a decrease of the translational velocity. Figure10 and figure11 shows the translational velocity with different values of Grashof number

(Gr) and modified Grashof number (Grc) respectively. It can be seen that an increase in Gr and Grc leads to rise in velocity profiles. For different values of the Schmidt number Sc, figure12 shows that the effect of increasing values of Sc results in a decreasing velocity distribution. Figure13 shows that the fluid velocity increase as time increases. Figure14 shows the effect of magnetic field parameter on microrotation profiles across the boundary layer and as the magnetic field parameter decreases, the microrotation profiles decrease. This result shows that the magnitude of the microrotation on the porous plate decreases as M decreases. Figure15 shows the effect of the parameter n on the microrotation profiles. It is observed that the magnitude of microrotation decreases for increasing value of n. Figure16 illustrates microrotation distribution across the boundary layer for different values of thermal radiation parameter Nr. Microrotation profiles increases with increase in thermal radiation parameter and as a result, the momentum boundary layer thickness increases. Figure17 depicts microrotation profiles for different values of refraction parameter. It can be seen from the figure that microrotation profiles increase with the increase values of the parameter h. Figure18 illustrates the variation in microrotation distribution across the boundary layer for different values of chemical reaction parameter (Kc). It is observed that microrotation profiles decreases during the generative reaction($Kc < 0$) and increases in the destructive reaction($Kc > 0$). Figure19 and figure20 illustrates microrotation profiles for different values of Grashof number(Gr) and modified Grashof number (Grc) respectively. Increase in Gr or Grc leads to decrease in microrotation profiles. For different values of Schmidtl number (Sc), microrotation profiles is plotted in figure21. The result shows that microrotation profiles increases with increase in Schimdtl number.

Variation of temperature profiles for different values of thermal radiation parameter Nr is shown in figure22. The results show that the temperature profiles increases with increase in the thermal radiation parameter and hence there would be an increase of thermal boundary layer thickness. Figure23 shows the variation of the temperature profiles for different values of the Pr. The result shows that an increase of the Pr results in a decrease in the thermal boundary layer thickness and a uniform temperature distribution across the boundary layer. The reason is that the smaller values of Pr are equivalent to increasing the thermal conductivities and therefore heat is able to diffuse away from the heated surface more rapidly

than for larger values of Pr. Hence the thicker the boundary layer is, the slower the rate of heat transfer is. Figure24 indicates that there is a decrease in temperature as time increases. The concentration profiles for different values of chemical reaction parameter is shown in figure25. There is a fall in the concentration due to the increasing values of the chemical reaction parameter. This shows that the diffusion rates can be tremendously altered by chemical reaction. Figure26 shows the concentration profiles for various values of Sc. It is observed that an increase in Sc leads to a decrease in the concentration distribution, because the smaller values of Sc are equivalent to an increase in the chemical molecular diffusivity. Figure27 shows the variation of concentration distribution across the boundary layer for different values of Soret number Sr.The concentration of the fluid increases with increase in the Soret parameter. Figure28 illustrates that the solute concentration in the fluid decrease as time increases.

Table1 shows the effect of Sc, Nr, Kc, and Sr on the skin friction coefficient Cf. It is observed that increase in Kc and Sc decreases the skin friction coefficient while Nr and Sr increases the skin friction coefficient. Table2 depicts the effect of Sc, Nr, Kc and Sr. It is also observed from the table that increase in Kc and Sc decreases the couple stress coefficient while Nr and Sr increases the couple stress coefficient. Table3 shows the effect of Pr and Nr on the Nusselt number Nu. The Nusselt number increases with increase in Pr. This shows that the surface heat transfer from the porous plate increases with the increasing values of the Pr. And the Nu decreases with increase in Nr. Table4 indicates the effect of Kc and Sc on Sherwood number Sh. It is noticeable that with an increase in Kc or Sc, the rate of mass transfer increases. Table5 illustrates the variation of the coefficient of skin friction, heat transfer and mass transfer with various values of time. The table shows that skin friction and heat transfer increase with time while mass transfer decrease with time. These results are in good agreement with the result of Chaudhary[27] and Rawa [2].

6. CONCLUSION

The problem of unsteady free convection MHD heat and mass transfer flow of an incompressible micropolar fluid past a semi-infinite vertical plate embedded in a porous medium with suction in the presence of thermal-diffusion and thermal radiation was studied.

The resulting partial differential equations which describe the problem, are transformed to dimensionless equations using dimensioless variables. These system of equations were solved analytically by using perturbation technique. The results are discussed through graphs and tables for different values of parameters entering into the problem. The following conclusions can be drawn from the results obtained:

*The translational velocity decreases with increase in the value of M, $K_c(Kc > 0)$, Pr, and Sc while it increases with an increasing n, Nr, Sr, K, h, $K_c(Kc < 0)$, Gr and Grc.

*The magnitude of microrotation decreases with an increasing n, Gr and Grc while the reverse effect is seen with an increase M, Nr, h, Kc and Sc.

*The temperature profile increases with an increasing value Nr whereas the effect is opposite for Pr and Kc.

*The concentration of the fluid decreases as Sc increases while reverse effect is seen with an increase in Sr.

DEDICATION

This paper is written to acknowledge the contributions of Professor R. O. Ayeni to the growth of study and learning of Mathematics in Nigeria

NOMENCLATURE

B_0	magnetic flux density
n	parameter related to microgyratio vector and shear stress
C	concentration
N	model parameter
Cf	skin friction coefficient
Nu	Nusselt number
Cm	couple stress coefficient
P	pressure
C_p	specific heat at constant pressure
Pr	Prandtl number
D	chemical molecular diffusivity
Sc	Schmidt number
g	acceleration due to gravity
Sh	Sherwood number
h	refraction parameter
t	time
Grc	modified Grashof number
T	temperature
G_r	Grashof number

u, v	components of velocities
j	microinertia per unit mass
U_0	scale of free stream velocity
k	thermal conductivity
V_0	scale of suction velocity
K	permeability of the porous medium
x ,y	distance along and perpendicular to the plate
M	magnetic field parameter
K_c	chemical reaction parameter
m_1	Maxwell's reflection coefficient
q_r	radiative heat flux
Nr	radiation parameter
Sr	Soret number
L	mean free path

GREEK SYMBOL

α	fluid thermal diffusivity
μ	fluid dynamic viscosity
β	ratio of vortex viscosity and dynamic viscosity
ρ	fluid density
β_c	coefficient of volumetric expansion with concentration
σ	electrical conductivity
β_f	coefficient of volumetric expansion of the working fluid
ν	fluid kinematic viscosity
γ	spin gradient viscosity
ν_r	fluid kinematic rotational viscosity
δ	scalar constant
w	angular velocity vector
ϵ	scalar constant($\epsilon \ll 1$)
θ	dimensionless temperature
$\wedge$	coefficient of vortex viscosity

REFERENCES

[1] Sunil, A. Sharma, A. Bharti, P.K. and Shandi, R.G. Effect of rotation on a layer of micropolar ferromagnetic fluid heated from below saturating a porous medium, International Journal of Engineering science, vol. 44 no. 11-12, pp. 683-698, 2006..

[2] Rawat, S. and Bhargava, R. Finite element study of natural convection heat and mass transfer in a micropolar fluids-saturated porous regime with Soret/Dufour effects Int.J. of Appl. Maths and mech. 5(2): 58-71, 2009

[3] Patil, P.M. and Kulkarni P.S. Effects of chemical reaction on free convective flow of a polar fluid through a porous medium in the presence of internal heat generation, Int.Therm. Sci. 4. Pp. 1043-1054,2008

[4] Rahman, M.A. and Sattar, M.A. Transient convective flow of micropolar fluid past a continuously moving vertical porous plate in the presence of radiation, International Journal of Applied Mechanics and Engineering, vol.12, no. 2 pp.497-513, 2007.

[5] Keelson, N.A., Desseaux, A. Effects of surface condition on flow of a micropolar fluid driven by a porous stretching sheet, Int. J. Eng. Sci, 39, pp. 1881-1897, 2001.

[6] Eldabe, N.T. and Ouat, M.E., Chebyshew finite difference method for heat and mass transfer in hydromagnetic flow of a micropolar fluid past a stretching surface with Ohmic heating and viscous dissipation, Appl. Math. Comput., 177, pp. 561-571, 2006.
[7] Mahmoud, M.A.A., Thermal radiation effects on MHD flow of a micropolar fluid over a stretching surface with variable thermal conductivity, Physical A. 375, pp. 401-410, 2007..
[8] Reena- I. and Rana U.S., Linear stability of thermo solutal convection in a micropolar fluid saturating a porous medium, International Journal of Application and Applied mathematics, vol. 4, no. 1 pp.62-87 2009
[9] Rehbi, A.D., Tariq, A.A. Benbella, A.S. Mahoud, A.A. Unsteady natural convection heat transfer of micropolar fluid over a vertical surface with constant Heat flux, Turkish J. Eng. Env. Sci. Vol. 31, pp. 225-233 (2007).
[10] Magdy, A.C., Free convection flow of conducting micropolar fluid with thermal relaxation including heat sources, Journal of Applied Mathematics, Vol. 2, 70.4 pp.271-292,2005.
[11] Brewster, M. Q., Thermal radiation transfer properties, John Wiley and sons,12:6-9, 1972.
[12] Srinivasacharya.D., Ramreddy. C.,Soret and Dufour effect on mixed convection in a non-Darcy porous medium saturated with micropolar fluid, Non-analysis modelling and control, vol.16,No.1, 100-115,2011.
[13] Cogley A.C., Vincent W.E., Gilles S.E.Differential approximation for radiation in a non-gray gas near equilibrium. AIAAJ. 6:551-553,1968.
[14] Erigen A.C, Theory of micropolar fluids J. math.mech. 16, pp.1-18,1966.
[15] Olajuwon. B.I. Convection heat and mass transfer in a hydromagnetic flow of a second grade fluid in the presence of thermal radiation and thermal diffusion. Int. commu. Heat and mass 38:377-382,2008
[16] Satter M.D. A, Hamid M.D. K. Unsteady free convection interaction with thermal radiation in a boundary layer flow past a vertical porous plate. Jour. Math. Phys. Sci. 30:25-37, 1996
[17] Hossain MA, Takhar Hs. Radiation effect on mixed convection along a vertical plate with uniform surface temperature, Heat mass transfer 31:243-248, 1996
[18] Makinde OD Free convection flow with thermal radiation and mass transfer past a moving vertical porous plate. Int. comm.Heat mass transfer, 25:289-295, 2005
[19] Das K, Jana S.Heat and mass transfer effects on unsteady MHD free convection flow near a moving vertical plate in a porous medium. Bull. Soc. Banja luka 17:15-32,2010
[20] Haque Md Z, Alam Md M, Ferdows M, Postelnicu A. Micropolar fluid behaviors on steady MHD free convection flow and mass transfer with constant heat and mass fluxes, joule heating and viscous dissipation. J.King Saud Univ. Engg.Sci doi:10.1016/j.jksues.2011.02.003, 2011.
[21] Modather M, Rashad A.M, Chamkha A.J. Study of MHD heat and mass transfer oscillatory flow of a micropolar fluid over a vertical permeable plate in a porous medium. Turkis J. eng. Env. Sci. vol33, 245-257, 2009.
[22] Kandasamy R., Periasamy K. and Sivagnana K. Chemical reaction, heat and mass transfer on MHD flow over a vertical stretching surface with heat source and stratification effects. Int. J. of heat and mass transfer, 48, 4557, 2005.
[23] Mohamad. Double diffusive convection-radiation interaction on unsteady MHD flow over a vertical moving porous plate with heat generation and soret effect, Applied mathematical sciences 13, pp. 629-651, 2009
[24] Ganapathy R. A note on oscillatory coquette flow in a rotating system. ASME J. Appl. Mech. 61; 208-209, 1994.

[25] Khedr M. E. , Chamkha A. J. and Bayomi M. MHD flow of a micropolar fluid past a stretched permeable surface with heat generation or absorption. Non-linear analysis modeling and control. Vol. 14, no 1, 27-40

[26] Seddek M.A. Finite-element method for effects of chemical reaction, variable viscosity, thermophoresis and heat generation/absorption on a boundary layer hydromagnetic flow with heat and mass transfer over a heat surface. Acta mech. 177,pp. 1-18,2005

[27] Chaudhary, R.C. and Abhay K.J . Effect of chemical reaction on MHD micropolar fluid flow past a vertical plate in slip-flow regime. Appl. Math. Mech. Engl. Ed. 29(9): 117-1194, 2008

[28] Rees, D. A and Bassom A. P. The Blasisum boundary layer flow of micropolar fluid. Int. Engng. Sci, 34: 113-124, 1996

DEPARTMENT OF MATHEMATICS, UNIVERSITY OF PORT HARCOURT, PORT HARCOURT, NIGERIA.
E-mail address: imumolen@yahoo co.uk

DEPARTMENT OF MATHEMATICS, FEDERAL UNIVERSITY OF AGRICULTURE, ABEOKUTA, NIGERIA
E-mail address: olajuwonishola@yahoo.com

DEPARTMENT OF MECHANICAL ENGINEERING, FEDERAL UNIVERSITY OF AGRICULTURE, ABEOKUTA, NIGERIA
E-mail address: waheedma@funaab.edu.ng

DEPARTMENT OF MATHEMATICS, FEDERAL UNIVERSITY OF AGRICULTURE, ABEOKUTA, NIGERIA
E-mail address: abialaio@funaab.edu.ng